

---

## Coordinated Control of SVC and PSS for Transient Stability Enhancement of Multi-Machine Power System

Lin Xu

Sichuan Electric Power Research Institute, No.24, Qinghua Road, Qingyang District, 610072 Chengdu, China

Corresponding author, e-mail: xulin198431@hotmail.com

### Abstract

*The coordinated control for SVC and generic/multi-band PSS for power swing damping is presented for the multimachine power system. The background and the mathematical models of the generic PSS, the multi-band PSS and the SVC are presented. The V-I characteristics as well as the dynamic properties of the static var compensator (SVC) are presented. The multi-machine power system is simulated using MATLAB and the effect of PSS and SVC on dynamic response of the system under single-phase fault and three-phase fault are simulated. The simulation results reveal that the coordinated control of the SVC and the generic/multi-band PSS is an effective solution to damp low frequency oscillation for multimachine power system and enhance global stability of the large inter-connected power system.*

**Keywords:** *the static var compensator (SVC), power system stabilizer (PSS), generic PSS, multi-band PSS, coordinated control, lower frequency oscillation*

**Copyright © 2013 Universitas Ahmad Dahlan. All rights reserved.**

### 1. Introduction

The basic intent of adding a Power System Stabilizer (PSS) is to enhance damping to extend the power transfer limits. The very nature of a PSS limits its effectiveness to small excursions about a steady state operating point [1]. The small excursions about an operating point are typically the result of an electrical system that is lightly damped which can cause spontaneous growing oscillations, known as system modes of oscillation. Enhanced damping is required when a weak transmission condition exists along with a heavy transfer of load. In the WECC, inter-area modes of oscillation occur between 0.1 and 1.0Hz. with the predominant mode at approximately 0.3Hz [1-4].

A PSS works in conjunction with the excitation system of a synchronous machine to modify the torque angle of the shaft to increase damping. The performance of the excitation system is critical in the overall capability of a PSS. Tuning of a PSS shall only be accomplished after the excitation system has been tuned and calibrated [5]. On new equipment, PSS may be software incorporated in digital automatic voltage regulators. AVR terminal voltage and current measurements are used to compute accelerating power and synthetic speed (integral of accelerating power). PSS cost can be low if PSS is required in competitive power plant procurement specifications. Procurement specifications should include requirement for tuning during commissioning and a requirement for stability program model and data [5, 6].

PSS are designed with various types of inputs. They include speed, frequency, power, accelerating power and integral of accelerating power. The PSS may derive these quantities from generator terminal voltage and current measurements. Current practice is to digitally derive a synthetic speed measurement (integral of accelerating power) from generator terminal voltage and current measurements. There is an interrelationship between the phase compensation and the washout time constant [1, 5, 6, 7]. Short washout time constants provide additional phase compensation in frequency-based PSS at the lower frequencies while dramatically reducing the gain. A washout time constant of 10 seconds or less is recommended to quickly remove low frequency components (below 0.1Hz) from the PSS output. The smaller time constant will reduce the influence on the system voltage from the PSS during any sustained/extended frequency deviation (i.e., loss of generation), especially if the PSS has a high gain setting [7, 8].

On the other hand, the static var compensator (SVC) is a shunt device of the Flexible AC Transmission Systems (FACTS) family using power electronics to control power flow and improve transient stability on power grids [1, 3, 9]. The SVC regulates voltage at its terminals by controlling the amount of reactive power injected into or absorbed from the power system. When system voltage is low, the SVC generates reactive power (SVC capacitive). When system voltage is high, it absorbs reactive power (SVC inductive) [10, 11].

This paper presents the coordinated control for SVC and PSS for power swing damping for the multimachine power system. Firstly, the background of the PSS and SVC is introduced, and the mathematical models of these controllers are also presented. In Section 2, the generic PSS and the multi-band PSS are introduced and compared. In Section 3, the static var compensator (SVC) is discussed, the V-I characteristics as well as the dynamic properties are presented. In Section 4, the multi-machine power system is simulated using MATLAB and the effect of PSS and SVC on dynamic response of the system under single-phase fault and three-phase fault are simulated. Section 5 concludes this paper.

## 2. Power System Stabilizer (PSS) Models

### 2.1. Generic Power System Stabilizer

The generic power system stabilizer (PSS) block can be used to add damping to the rotor oscillations of the synchronous machine by controlling its excitation. The disturbances occurring in a power system induce electromechanical oscillations of the electrical generators. These oscillations, also called power swings, must be effectively damped to maintain the system stability [1, 3, 4].

The output signal of the PSS is used as an additional input ( $v_{stab}$ ) to the Excitation System block. The PSS input signal can be either the machine speed deviation,  $d\omega$ , or its acceleration power,  $P_a = P_m - P_{eo}$  (difference between the mechanical power and the electrical power) [1, 5-8].

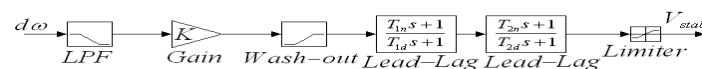


Figure 1. The Block Diagram of the Generic Power System Stabilizer

Figure 1 shows the block diagram of the generic power system stabilizer (PSS), which can be modeled by using the following transfer function [1]:

$$G(s) = K \cdot \frac{T_{1n}s + 1}{T_{1d}s + 1} \cdot \frac{T_{2n}s + 1}{T_{2d}s + 1} \quad (1)$$

To ensure a robust damping, the PSS should provide a moderate phase advance at frequencies of interest in order to compensate for the inherent lag between the field excitation and the electrical torque induced by the PSS action. The model consists of a low-pass filter, a general gain, a washout high-pass filter, a phase-compensation system, and an output limiter. The general gain  $K$  determines the amount of damping produced by the stabilizer [1, 3, 4].

The washout high-pass filter eliminates low frequencies that are present in the  $d\omega$  signal and allows the PSS to respond only to speed changes. The phase-compensation system is represented by a cascade of two first-order lead-lag transfer functions used to compensate the phase lag between the excitation voltage and the electrical torque of the synchronous machine.

### 2.2. Multi-band Power System Stabilizer

The disturbances occurring in a power system induce electromechanical oscillations of the electrical generators. These oscillations, also called power swings, must be effectively damped to maintain the system's stability. Electromechanical oscillations can be classified in four main categories [1, 3, 4]:

- (1) Local oscillations: between a unit and the rest of the generating station and between the latter and the rest of the power system. Their frequencies typically range from 0.8 to 4.0Hz.
- (2) Interplant oscillations: between two electrically close generation plants. Frequencies can vary from 1 to 2Hz.
- (3) Interarea oscillations: between two major groups of generation plants. Frequencies are typically in a range of 0.2 to 0.8Hz.
- (4) Global oscillation: characterized by a common in-phase oscillation of all generators as found on an isolated system. The frequency of such a global mode is typically under 0.2Hz.

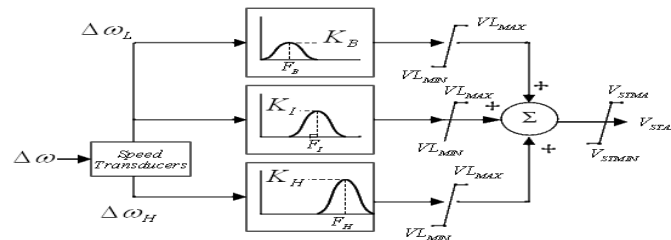


Figure 2. The Block Diagram of the Multi-band Power System Stabilizer (MB-PSS)

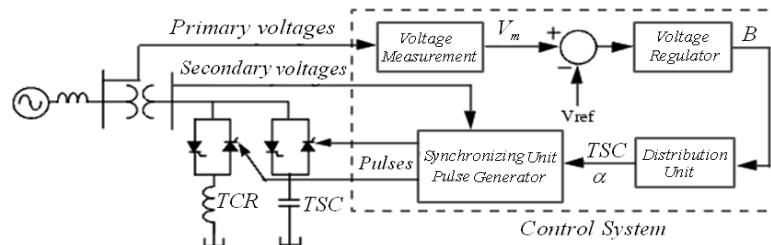


Figure 3. The Single-Line Diagram of a Static Var Compensator and its Control System.

The need for effective damping of such a wide range, almost two decades, of electro-mechanical oscillations motivated the concept of the multiband power system stabilizer (MB-PSS), as shown in Figure 2. Just as its name reveals, the MB-PSS structure is based on multiple working bands. Three separate bands are dedicated to the low-, intermediate-, and high-frequency modes of oscillations: the low band is typically associated with the power system global mode, the intermediate with the interarea modes, and the high with the local modes.

Each of the three bands is made of a differential bandpass filter, a gain, and a limiter. The outputs of the three bands are summed and passed through a final limiter producing the stabilizer output  $V_{stab}$ . This signal then modulates the set point of the generator voltage regulator so as to improve the damping of the electromechanical oscillations. To ensure robust damping, the MB-PSS should include a moderate phase advance at all frequencies of interest to compensate for the inherent lag between the field excitation and the electrical torque induced by the MB-PSS action.

### 3. Static Var Compensator (SVC)

Figure 3 shows the single-line diagram of a static var compensator and its control system. The variation of reactive power is performed by switching three-phase capacitor banks and inductor banks connected on the secondary side of a coupling transformer. Each capacitor bank is switched on and off by three thyristor switches (Thyristor Switched Capacitor or TSC). Reactors are either switched on-off (Thyristor Switched Reactor or TSR) or phase-controlled (Thyristor Controlled Reactor or TCR) [1, 3, 4-8].

The control system consists of the following issues:

- (1) A measurement system measuring the positive-sequence voltage is to be controlled.
- (2) A Fourier-based measurement system using a one-cycle running average is used.

- (3) A voltage regulator that uses the voltage error (difference between the measured voltage  $V_m$  and the reference voltage  $V_{ref}$ ) to determine the SVC susceptance  $B$  needed to keep the system voltage constant.
- (4) A distribution unit that determines the TSCs (and eventually TSRs) must be switched in and out, and computes the firing angle of TCRs.
- (5) A synchronizing system using a phase-locked loop (PLL) synchronized on the secondary voltages and a pulse generator that send appropriate pulses to the thyristors

### 3.1. SVC V-I Characteristic

The SVC can be operated in two different modes: In voltage regulation mode (the voltage is regulated within limits as explained below). In var control mode (the SVC susceptance is kept constant). When the SVC is operated in voltage regulation mode, it implements the following V-I characteristic (Figure 4) [1].

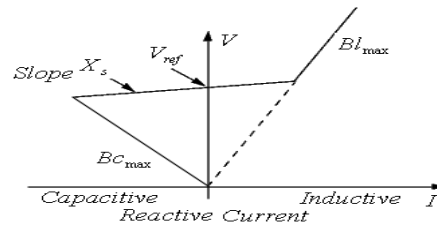


Figure 4. The V-I Characteristics of the SVC

As long as the SVC susceptance ( $B$ ) stays within the maximum and minimum susceptance values imposed by the total reactive power of capacitor banks ( $B_{c_{max}}$ ) and reactor banks ( $B_{l_{max}}$ ), the voltage is regulated at the reference voltage  $V_{ref}$ .

However, a voltage droop is normally used (usually between 1% and 4% at maximum reactive power output), and the V-I characteristic has the slope indicated in the Figure. The V-I characteristic is described by the following three equations [1, 3, 4]:

$$V = V_{ref} + X_s \cdot I, \text{ SVC is in regulation range } (-B_{c_{max}} < B < B_{l_{max}}) \quad (2)$$

$$V = -\frac{I}{B_{c_{max}}}, \text{ SVC is fully capacitive } (B = B_{c_{max}}) \quad (3)$$

$$V = \frac{I}{B_{l_{max}}}, \text{ SVC is fully inductive } (B = B_{l_{max}}) \quad (4)$$

where ' $V$ ' denotes the positive sequence voltage (p.u.); ' $I$ ' denotes the reactive current (p.u./Pbase) (' $I$ '>0 indicates an inductive current); ' $X_s$ ' denotes the slope or droop reactance (p.u./Pbase); ' $B_{c_{max}}$ ' denotes the maximum capacitive susceptance (p.u./Pbase) with all TSCs in service, no TSR or TCR; ' $B_{l_{max}}$ ' denotes the maximum inductive susceptance (p.u./Pbase) with all TSRs in service, or TCRs at full conduction, no TSC.

### 3.2. SVC Dynamic Response

When the SVC is operating in voltage regulation mode, its response speed to a change of system voltage depends on the voltage regulator gains (proportional gain  $K_p$  and integral gain  $K_i$ ), the droop reactance  $X_s$ , and the system strength (short-circuit level). For an integral-type voltage regulator ( $K_p = 0$ ), if the voltage measurement time constant  $T_m$  and the average time delay  $T_d$  due to valve firing are neglected, the closed-loop system consisting of the SVC and the power system can be approximated by a first-order system having the following closed-loop time constant [1, 3, 4, 7]:

$$T_c = \frac{1}{K_i \cdot (X_s + X_n)} \tag{5}$$

where ' $T_c$ ' represents the closed-loop time constant; ' $K_i$ ' represents the proportional gain of the voltage regulator (p.u.\_B/p.u.\_V/s); ' $X_s$ ' represents the slope reactance p.u./Pbase; ' $X_n$ ' represents the equivalent power system reactance (p.u./Pbase).

This equation demonstrates that we obtain a faster response speed when the regulator gain is increased or when the system short-circuit level decreases (higher  $X_n$  values). If we take into account the time delays due to voltage measurement system and valve firing, we obtain an oscillatory response and, eventually, instability with too weak a system or too large a regulator gain.

#### 4. Simulation Results and Discussions

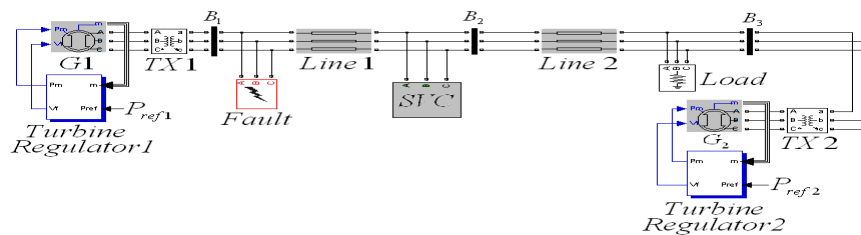


Figure 5. The Circuit Diagram of the Multi-Machine Power System with SVC and PSS

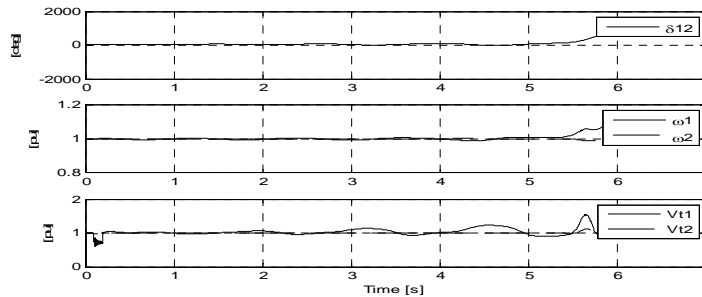


Figure 6. The Simulated Response of the Rotor Angle Difference  $\delta_{12}$ , Angular Speed  $\omega_1, \omega_2$ , and the Terminal Voltage  $V_{t1}, V_{t2}$  Under Single-Phase Fault Without SVC and PSS.

Table 1 shows the specification and parameters of the multi-maching power system. A 1000MW hydraulic generation plant (machine M1) is connected to a load center through a long 500kV, 700km transmission line. The load center is modelled by a 5000MW resistive load. The load is fed by the remote 1000MW plant and a local generation of 5000MW (machine M2). The system has been initialized so that the line carries 950MW which is close to its surge impedance loading (SIL=977MW). In order to maintain system stability after faults, the transmission line is shunt compensated at its center by a 200-Mvar static Var compenstor (SVC). Notice that this SVC model is a phasor model valid only for transient stability solution. The SVC does not have a power oscillation damping (POD) unit.

Table 1. The Specification and Parameters of the Multi-Matching Power System

Specification	System parameters
Load center	5000 MW, resistive load
Power plant 1 (G1)	1000 MW
Power plant 2 (G2)	5000 MW
Initial power flow	950 MW
Surge impedance loading (SIL)	977 MW
Power rating of SVC	200 MVar

The two machines are equipped with a hydraulic turbine and governor (HTG), excitation system and power system stabilizer (PSS). These blocks are located in the two turbine and regulator' subsystems. Two types of stabilizers can be selected: a generic model using the acceleration power ( $P_a$ =difference between mechanical power  $P_m$  and output electrical power  $P_{e0}$ ) and a Multi-band stabilizer using the speed deviation ( $\Delta\omega$ ).

#### 4.1. Effect of PSS Under Single-Phase Fault Without SVC

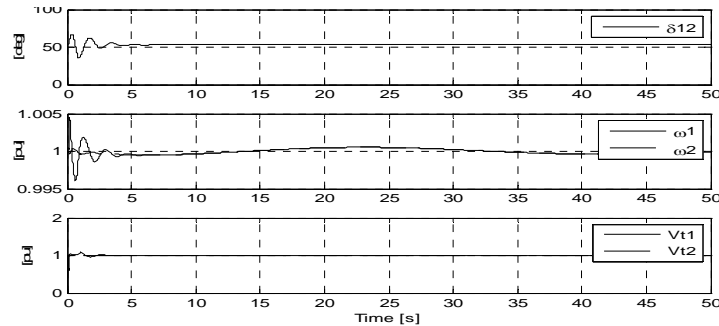


Figure 7. The Simulated Response of the Rotor Angle Difference  $\delta_{12}$ , Angular Speed  $\omega_1, \omega_2$ , and the Terminal Voltage  $V_{t1}, V_{t2}$  Under Single-Phase Fault Without SVC, With Generic PSS.

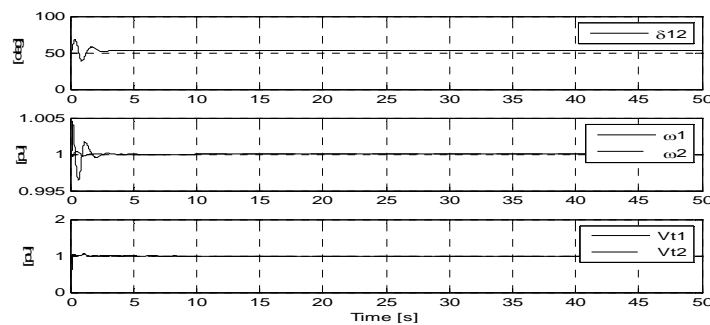


Figure 8. The Simulated Response of the Rotor Angle Difference  $\delta_{12}$ , Angular Speed  $\omega_1, \omega_2$ , and the Terminal Voltage  $V_{t1}, V_{t2}$  Under Single-Phase Fault Without SVC, With Multi-Band PSS.

Firstly, we test the effect of PSS under single-phase fault without SVC. The simulation results are summarized as follows:

Figure 6 shows the simulated response of the rotor angle difference  $\delta_{12}$ , angular speed  $\omega_1, \omega_2$ , and the terminal voltage  $V_{t1}, V_{t2}$  under single-phase fault without SVC and PSS. First trace shows the rotor angle difference  $\delta_{12}$  between the two machines. Power transfer is the maximum when this angle reaches 90 degrees, which is a good indication of system stability.

If  $\delta_{12}$  exceeds 90 degrees for a too long period of time, the machines will lose synchronism and the system instability is no longer sustained. Second trace shows the machine speeds. Notice that machine 1 speed increases during the fault because during that period its electrical power is lower than its mechanical power. It can be noticed that the system is unstable without PSS.

Figure 7 shows the simulated response of the rotor angle difference  $\delta_{12}$ , angular speed  $\omega_1, \omega_2$ , and the terminal voltage  $V_{t1}, V_{t2}$  under single-phase fault without SVC, with generic PSS. After fault clearing, the 0.8 Hz oscillation is quickly damped. This oscillation mode is typical of interarea oscillations in a large power system.

It can be noticed that the machine speeds oscillate together at a low frequency (0.025 Hz) after fault clearing. This extremely low frequency oscillation is characterized by a common in-phase oscillation of all generators as found on an isolated system, indicating the global oscillation mode.

Figure 8 shows the simulated response of the rotor angle difference  $\delta_{12}$ , angular speed  $\omega_1, \omega_2$ , and the terminal voltage  $V_{t1}, V_{t2}$  under single-phase fault without SVC, with multi-band PSS.

It can be observed that this multi-band PSS is capable to damp both the 0.8 Hz mode and the 0.025 Hz mode.

**4.2. Effect of PSS Under Three-Phase Fault Without SVC**

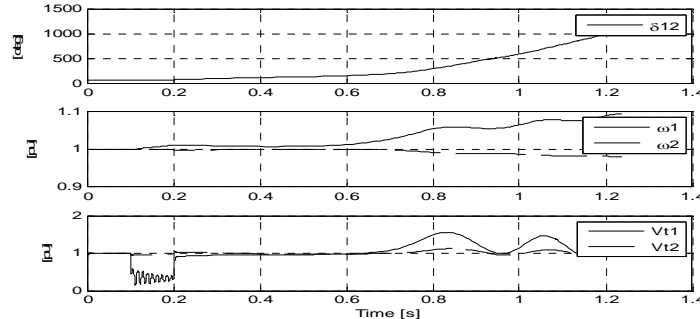


Figure 9. The Simulated Response of the Rotor Angle Difference  $\delta_{12}$ , Angular Speed  $\omega_1, \omega_2$ , and the Terminal Voltage  $V_{t1}, V_{t2}$  Under Three-Phase Fault Without SVC and PSS.

Next, we consider the effect of PSS under three-phase fault without SVC. Figure 9 shows the simulated response of the rotor angle difference  $\delta_{12}$ , angular speed  $\omega_1, \omega_2$ , and the terminal voltage  $V_{t1}, V_{t2}$  under three-phase fault without SVC and PSS. Figure 10 shows the simulated response of the rotor angle difference  $\delta_{12}$ , angular speed  $\omega_1, \omega_2$ , and the terminal voltage  $V_{t1}, V_{t2}$  under three-phase fault without SVC, with generic PSS.

Figure 11 shows the simulated response of the rotor angle difference  $\delta_{12}$ , angular speed  $\omega_1, \omega_2$ , and the terminal voltage  $V_{t1}, V_{t2}$  under three-phase fault without SVC, with multi-band PSS. It can be observed from Figures.9-11, that without SVC, the PSS is incapable to damp the system oscillation. The system remains unstable under both the generic PSS and the multi-band PSS.

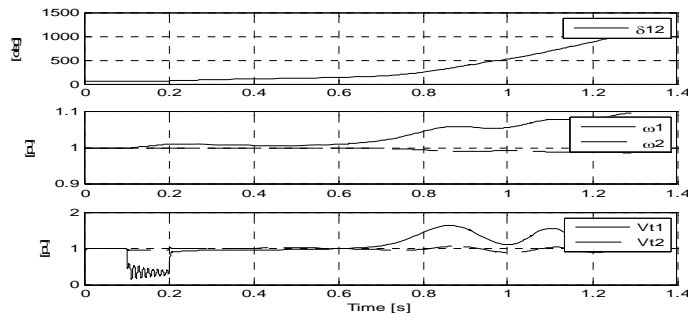


Figure 10. The Simulated Response of the Rotor Angle Difference  $\delta_{12}$ , Angular Speed  $\omega_1, \omega_2$ , and the Terminal Voltage  $V_{t1}, V_{t2}$  Under Three-Phase Fault Without SVC, With Generic PSS.

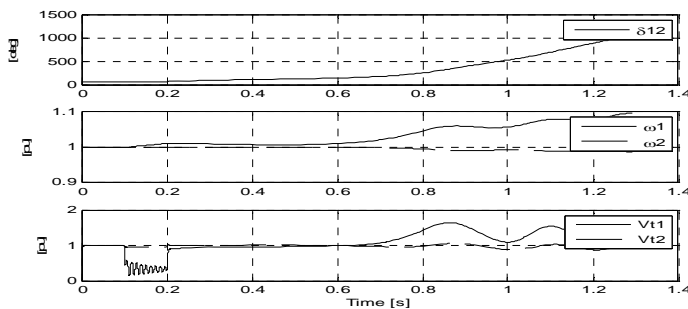


Figure 11. The Simulated Response of the Rotor Angle Difference  $\delta_{12}$ , Angular Speed  $\omega_1, \omega_2$ , and the Terminal Voltage  $V_{t1}, V_{t2}$  Under Three-Phase Fault Without SVC, With Multi-Band PSS.

### 4.3. Effect of PSS under Three-Phase Fault with SVC

Finally, we consider the effect of PSS under three-phase fault with SVC. Figure 12 shows the simulated response of the rotor angle difference  $\delta_{12}$ , angular speed  $\omega_1, \omega_2$ , and the terminal voltage  $V_{t1}, V_{t2}$  under three-phase fault with SVC and generic PSS. After fault clearing, the 0.8 Hz oscillation is quickly damped. This oscillation mode is typical of interarea oscillations in a large power system. It can be noticed that the machine speeds oscillate together at a low frequency (0.025 Hz) after fault clearing.

Figure 13 shows the simulated response of the rotor angle difference  $\delta_{12}$ , angular speed  $\omega_1, \omega_2$ , and the terminal voltage  $V_{t1}, V_{t2}$  under three-phase fault with SVC and multi-band PSS.

It can be observed from Figures.9-11, that without SVC, the PSS is incapable to damp the system oscillation. The system remains unstable under both the generic PSS and the multi-band PSS. It can be observed that this multi-band PSS is capable to damp both the 0.8 Hz mode and the 0.025 Hz mode.

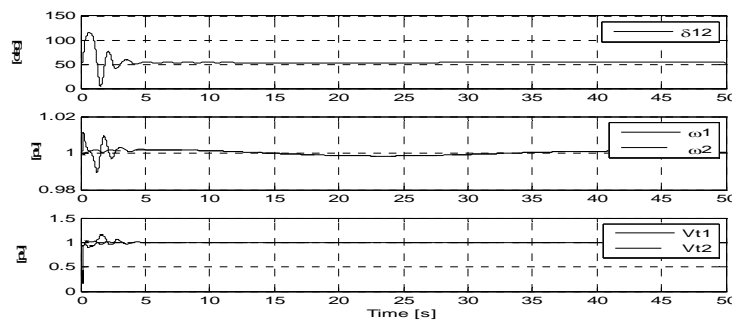


Figure 12. The Simulated Response of the Rotor Angle Difference  $\delta_{12}$ , Angular Speed  $\omega_1, \omega_2$ , and the Terminal Voltage  $V_{t1}, V_{t2}$  under Three-Phase Fault with SVC and Generic PSS.

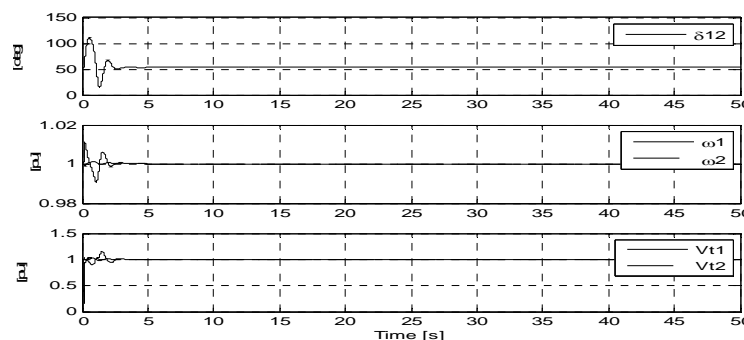


Figure 13. The Simulated Response of the Rotor Angle Difference  $\delta_{12}$ , Angular Speed  $\omega_1, \omega_2$ , and the Terminal Voltage  $V_{t1}, V_{t2}$  under Three-Phase Fault with SVC and Multi-Band PSS.

## 5. Conclusions

This paper presents the coordinated control for SVC and PSS for power swing damping for the multimachine power system. Firstly, the background of the PSS and SVC is introduced, and the mathematical models of these controllers are also presented. The generic PSS and the multi-band PSS are introduced and compared. The static var compensator (SVC) is discussed, the V-I characteristics as well as the dynamic properties are presented.

The multi-machine power system is simulated using MATLAB and the effect of PSS and SVC on dynamic response of the system under single-phase fault and three-phase fault are simulated. It can be concluded that the coordinated control of the SVC and the generic/multi-band PSS is an effective solution to damp low frequency oscillation for multimachine power system.

On the other hand, the SVC or PSS alone lacks the ability to damp oscillation under extreme grid disturbances. Hence, for the practical power system, the coordinated control of the SVC and multi-band PSS provides useful mean to enhance global electromechanical stability.



## References

- [1] P Kundur. Power System Stability and Control. New York: Mc-Graw-Hill, 1994.
- [2] N Mohan, TM Undeland, WP Robbins. Power Electronics: Converters, Applications and Design. New York: Wiley, 1995.
- [3] M Ilic, J Zaborszky. Dynamics and control of large electric power systems. New York: Wiley, 2000.
- [4] R Marconato. Electric Power Systems. Milan, Italy: CEI. 2008; 2.
- [5] Bhargava B, Dishaw G. Application of an energy source power system stabilizer on the 10MW battery energy storage system at Chino substation, *IEEE Transactions on Power Systems*.1998; 13(1):145-151.
- [6] Chaturvedi DK, Malik OP. Neurofuzzy power system stabilizer. *IEEE Transactions on Energy Conversion*. 2008; 23(3): 887-894.
- [7] H Wu, Tsakalis KS, Heydt GT. Evaluation of time delay effects to wide-area power system stabilizer design. *IEEE Transactions on Power Systems*. 2004; 19(4): 1935-1941.
- [8] Wu Chi-Jui, Hsu YuanYih, Design of self-tuning PID power system stabilizer for multimachine power systems. *IEEE Transactions on Power Systems*. 1998; 3(3): 1059-1064.
- [9] Sawa T, Shirai Y, Michigami T, Sakanaka Y, Uemura Y. A field test of power swing damping by static var compensator. *IEEE Transactions on Power Systems*. 1989; 4(3): 1115-1121.
- [10] Wang HF, Swift FJ. *Capability of the static var compensator in damping power system oscillations*. IEE Proceedings – Generation, Transmission and Distribution. 1996; 143(4) :353-358.
- [11] Chin-Hsing Cheng, Yuan-Yih Hsu, Damping of generator oscillations using an adaptive static var compensator. *IEEE Transactions on Power Systems*. 1992; 7(2): 718-725.